4. RESULTS AND DISCUSSION

This chapter Includes the results of different investigations, and their discussion. In this respect, the industrial solid sorbents (homra, fly ash, silica fume, ceramic and window glass.) were characterized using X-ray fluorescence, X-ray diffraction, and IR analysis as well as the capacity of each sorbent was investigated .

Essential parameters were studied mainly: effect of shaking time, effect of pH, effect of v/m , and effect of particle size. Also certain parameters that affect the cement pastes which contain the solid sorbents and that mixed with radioactive liquid waste were investigated mainly: the initial and final setting times, bleeding rate and bleeding capacity, curing time, water immersion, mechanical strength, and leachability (Rapid leaching and long term leachability test).

4.1. Characterization of the Industrial Solid Wastes:

4.1.1. Surface area:

The specific surface area (m^2/g) of the powdered solid waste materials (homra, fly ash, silica fume, ceramic and window glass.) were measured after their thermal treatment for 2 hours at 200^0C and the results obtained were listed in Table (6). The tabulated data indicate that, homra has the highest surface area values while window glass shows the lowest one.

Table (6): The specific surface area of thermally treated powders of the industrial waste material.

Material	Specific surface area, m^2/g
Homra	28.73
Fly ash	31.75
Silica fume	42.16
Ceramic	16.7
Window glass	12.85

4.1.2. X-ray fluorescence analysis:

X-ray fluorescence patterns of the industrial solid waste sorbents (homra, fly ash, silica fume, ceramic and window glass) were performed and their analysis obtained are presented in Table (7) which shows the chemical composition in weight percent (wt. %). The results indicated that, the main constituent of all solids is silica which consists about 94.7% in silica fume, about 68.63% in window glass, about 65.57 in ceramic, about 63.39% in homra and about 54% in fly ash.

Low contents were detected for K_2O (0.17%-1.18%), P_2O_5 (0.02%-0.98%), and TiO_2 (0.01%-0.98%) in all solids.

Table (7): Chemical compositions of industrial solid wastes (homra, fly ash, silica fume, ceramic and window glass) determined by X-ray fluorescence .

Compound	Homra, Wt.%	Fly ash, Wt.%	Silica fume, Wt.%	Ceramic, Wt.%	Window glass, Wt.%
SiO_2	63.39	54.05	94.70	65.35	68.63
Al_2O_3	17.78	10.58	0.52	21.43	1.33
Fe_2O_3	8.94	22.05	0.74	2.27	0.76
CaO	2.75	8.28	0.49	0.72	8.47
MgO	2.80	0.11	1.39	0.52	2.84
K_2O	1.18	0.19	1.10	0.96	0.17
Na_2O	1.93	2.98	0.89	7.61	17.53
P_2O_5	0.19	0.94	0.15	0.42	0.02
TiO_2	0.98	0.71	0.01	0.70	0.24
MnO	0.06	0.11	0.01	0.02	0.01

4.1.3. X-ray diffraction:

X-ray diffraction patterns of the investigated industrial solid wastes (homra, fly ash, silica fume, ceramic and window glass) were presented in Figs (3,4). The results indicate that, silica fume, fly ash, and window glass are amorphous (show no bands) but homra and ceramic show some crystalline pattern.

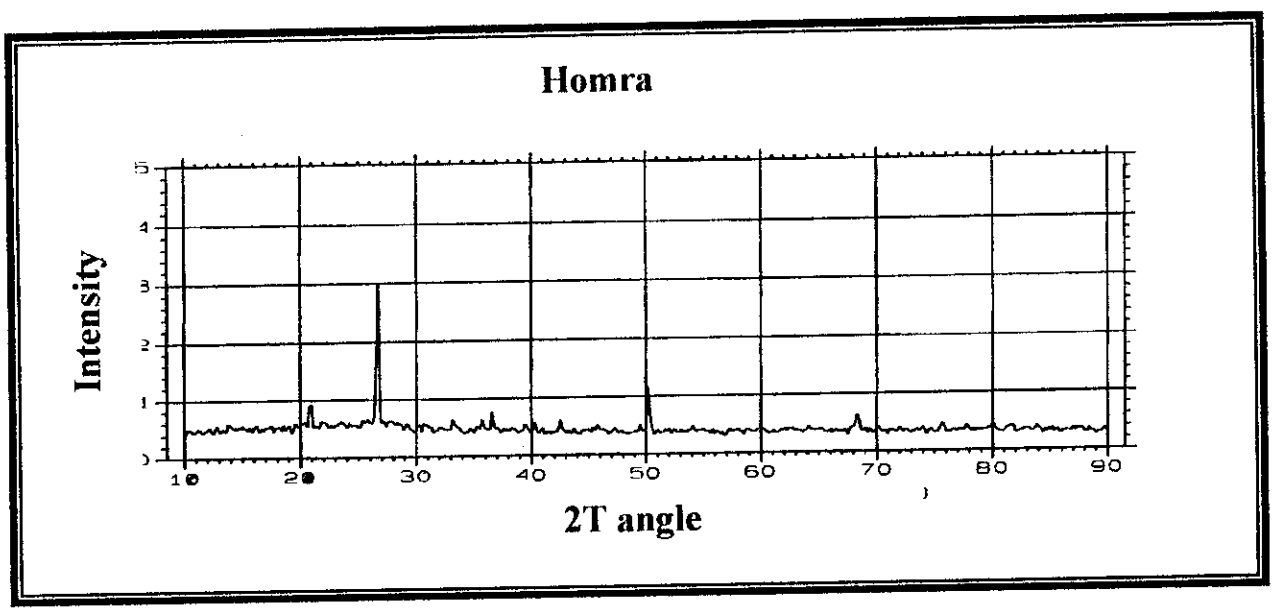

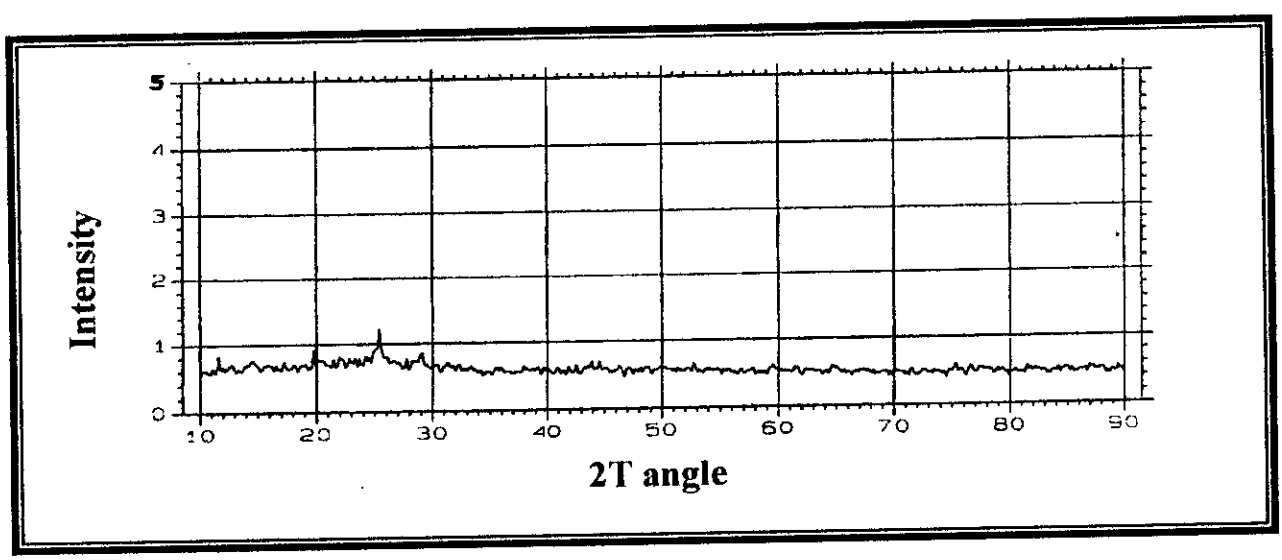

Fig. (3): X-ray diffraction patterns of homra and fly ash.

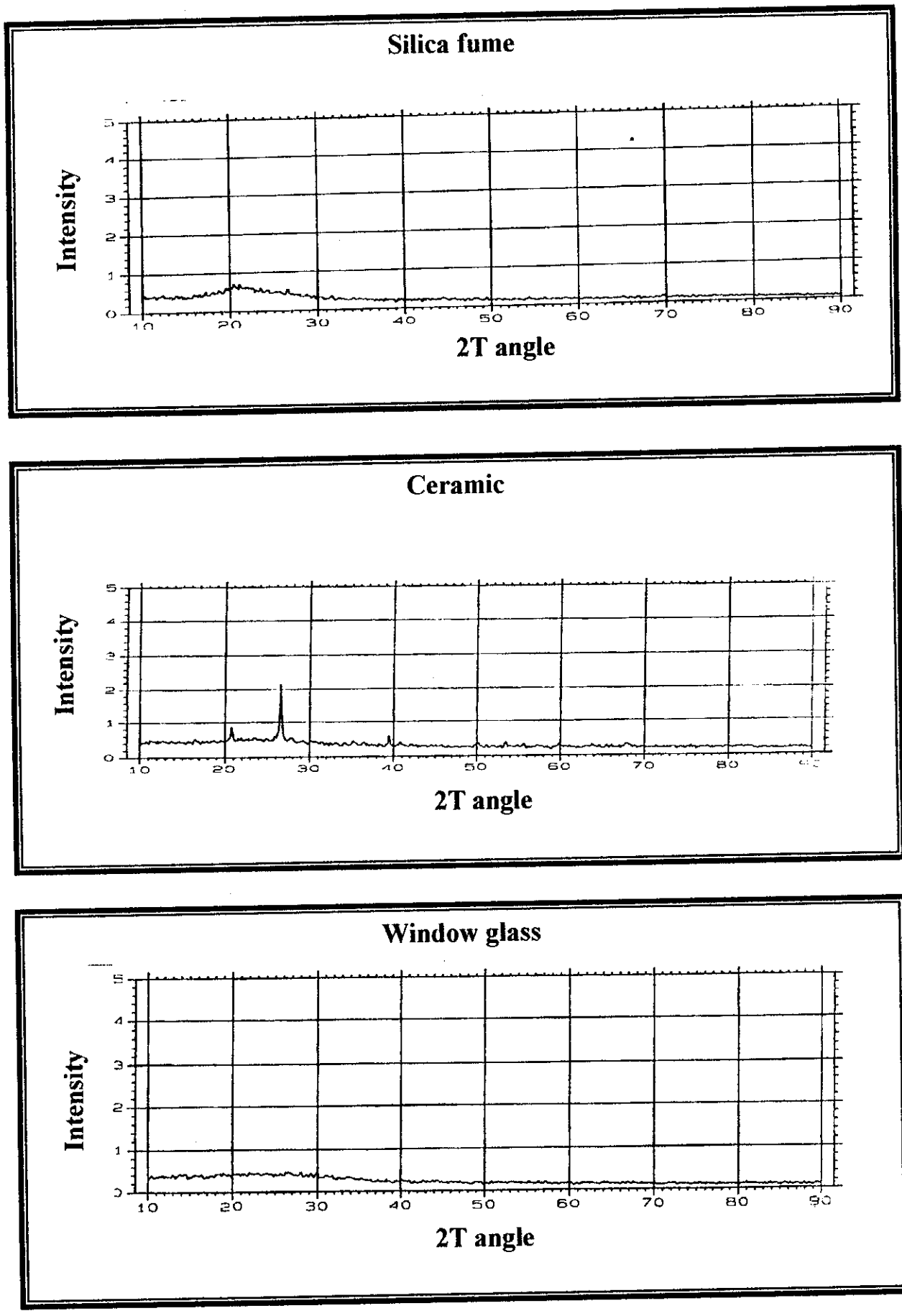

Fig. (4): X-ray diffraction pattern of silica fume, ceramic and window glass.

4.1.4 IR analysis:

The infrared spectroscopic investigations of the industrial solid wastes that used as sorbents (homra, fly ash, silica fume, ceramic and window glass) were measured and the spectra are shown in the region from 4000 to 600 cm^{-1} are presented in Figs (5,6).

The obtained spectra of the investigated sorbents were found to have a variety of bands that are diagnostic for the molecular structures. The samples yielded more or less similar infrared spectra with major bands at certain region.

Homra shows three bands, the first band is the weakest one at 3417 cm^{-1} which indicates a broad O-H absorption (**Stevenson 1982**). The second band is the strongest one at 1083 cm^{-1} which can be assigned as a C-O stretching and O-H bending deformation which is mainly due to various oxygenated groups (**Vili 1990**). The third band at 779 cm^{-1} which can be attributed to a ≡C-H out of plane bending.

Fly ash shows three bands also, the first band is the weakest one at 3330cm^{-1} . The second band at1629 cm^{-1} . The third band is the strongest one at 1119 cm^{-1} which assigned as a C-O stretching and O-H bonding.

Silica fume shows two strong bands, the first band at 1124 cm^{-1} assigned as a C-O stretching and O-H bonding. The second band at 800 cm^{-1} which is attributed to a ≡C-H .

Ceramic and window glass almost show the same bands, the first band at 3400 cm^{-1} is assigned as a H- bonded OH group. The second band at 1062 cm^{-1} is assigned as a C-O stretching and O-H bending (**Stevenson 1982**). The third band at 780 cm^{-1} can be attributed to a ≡C-H out-of plane bending.

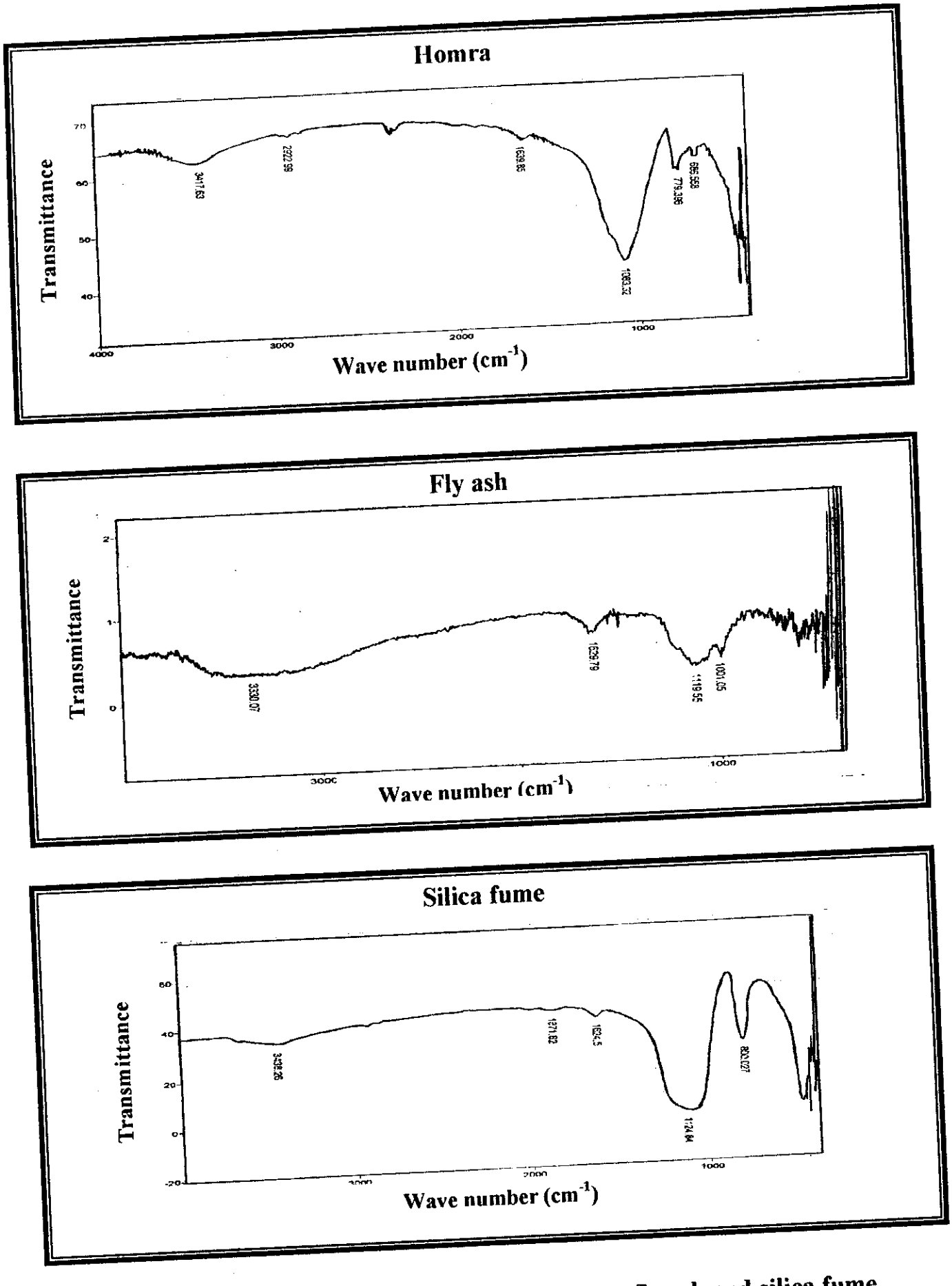

Fig. (5): Infrared spectroscopic patterns of homra, fly ash and silica fume.

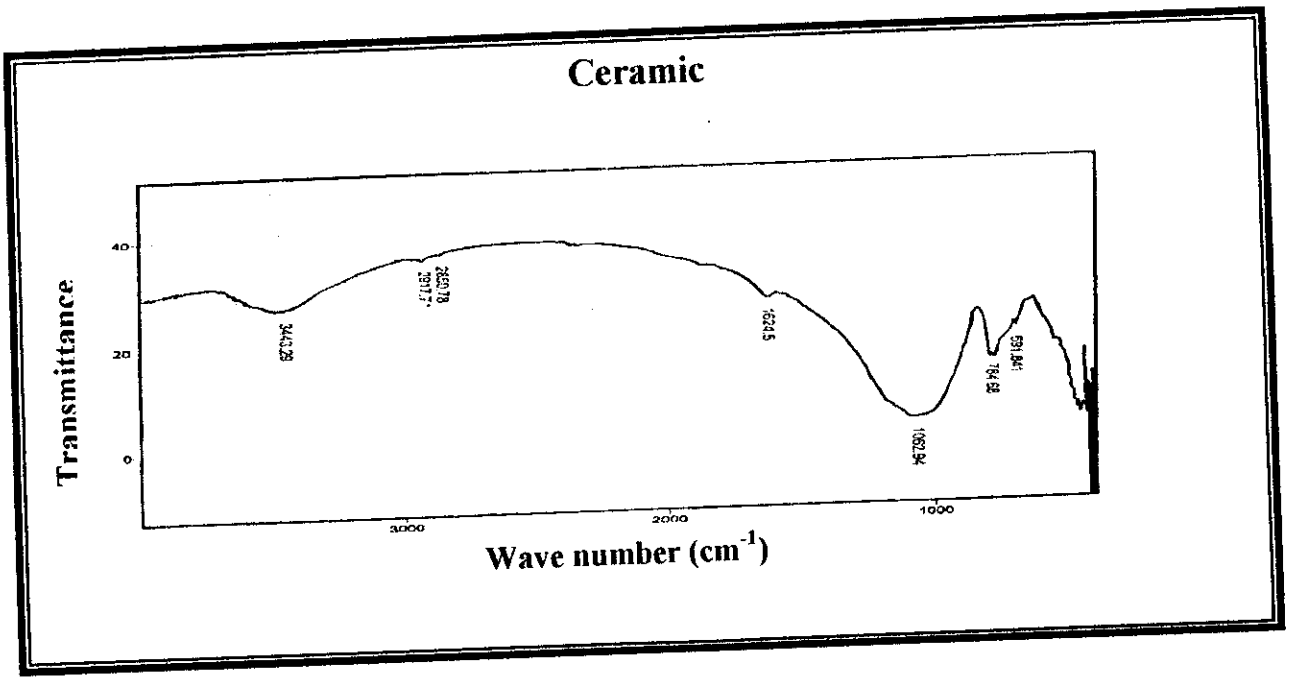

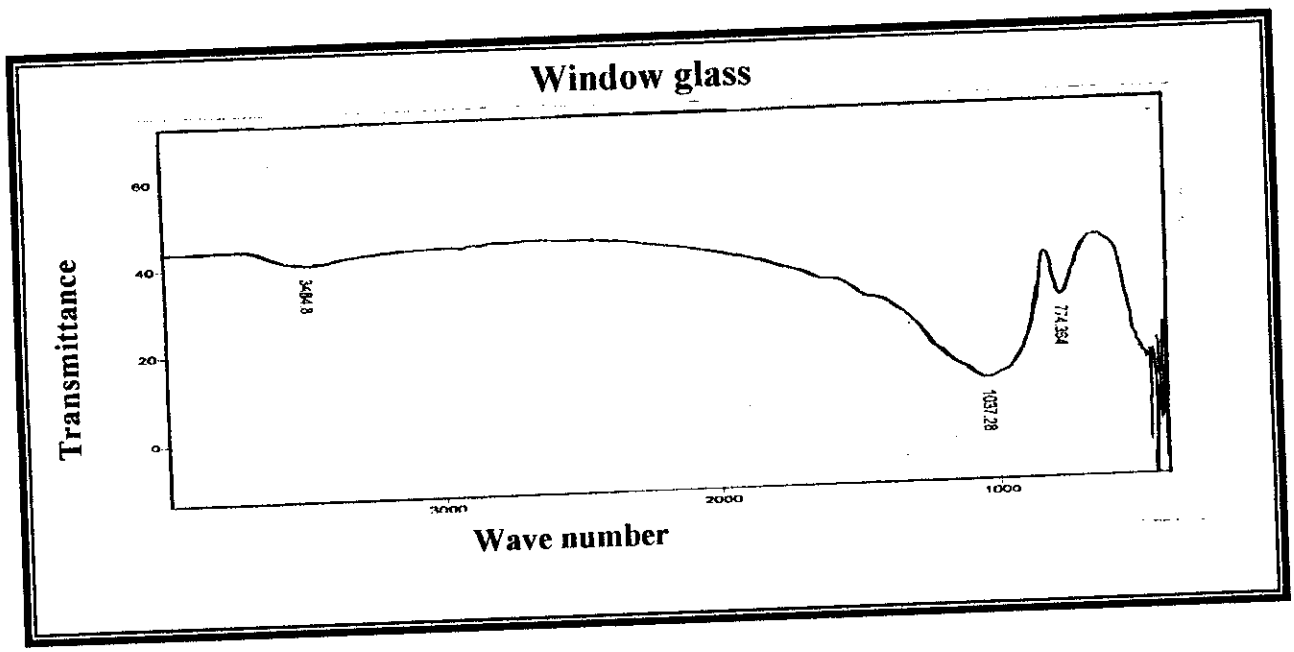

Fig. (6): Infrared spectroscopic patterns of ceramic and window glass.

4.2. Effect of shaking time:

Effect of shaking time on the uptake % of ^{137}Cs, ^{60}Co and $^{152\&154}Eu$ using 0.1mm of the industrial solid wastes: homra, fly ash, silica fume, ceramic and window glass as sorbents was evaluated at the ambient room temperature (25±1°C) and pH 8. The results obtained are listed in Tables (8-12).

From these data it can be concluded that the sorption of radioactive ions (Cs^+, Co^{2+} and Eu^{3+}) is initially quite fast and occurs within the first few minutes. The complete uptake was established after 40 minutes (equilibration time) for all ions with all the solids investigated. This can be mainly attributed to that: initially the ions preferentially occupied many of the active sites of the solids in a random manner, as a result of which the rate of uptake is fast. After prolonged period of time, most of the active sites are occupied with ions; hence the rate of sorption becomes slow in the later stages and ultimately approaches a plateau **(Juvani 1996).**

Window glass shows a high affinity toward the radioactive ions inspite of its small surface area, this may be attributed to its alkali phases and its pore diameter **(Jawed and Skalny 1978).**

Also from Figs (7-11) it is clear that, Eu^{3+} has the greatest values of the uptake values rather than that of cesium or cobalt with all solids which may be attributed to their ionic size $Eu^{3+} < Co^{2+} < Cs^+$ **(Abdelraouf et al 1997)** for all the solids used, the uptake percentages of Cs^+, Co^{2+} and Eu^{3+} are arranged according to the following sequence: $Eu^{3+} > Co^{2+} > Cs^+$.

Table (8): Effect of shaking time on the uptake % of ^{137}Cs, ^{60}Co and $^{(152+154)}Eu$ from the radioactive liquid waste on homra at the ambient room temperature (25±1°C) and pH 8 .

Time, min	Uptake, %		
	Cs^{+}	Co^{2+}	Eu^{3+}
5	78.0	79.9	82.2
10	84.0	86.0	89.6
20	88.2	90.1	94.9
30	91.8	92.7	96.6
40	92.9	94.1	98.9
60	92.6	94.2	98.9
90	92.9	93.8	99.2
120	92.8	93.9	99.1
150	92.9	94.0	99.1
180	93.06	94.2	99.0
210	93.1	94.2	99.0

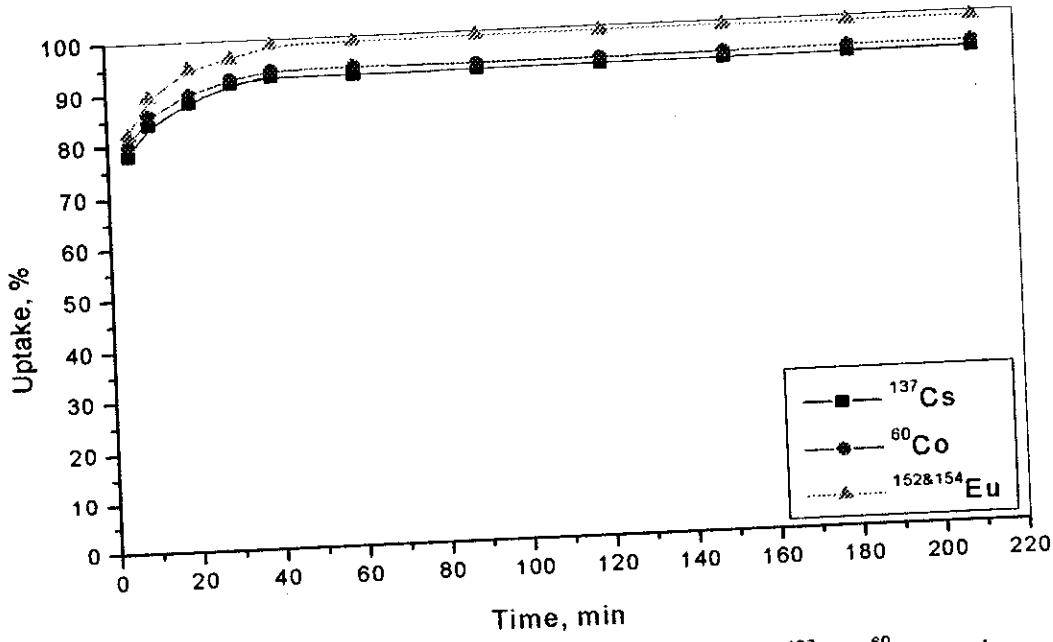

Fig. (7): Effect of shaking time on the uptake% of ^{137}Cs, ^{60}Co and $^{152,154}Eu$ from the radioactive liquid waste on homra.

Table (9): Effect of shaking time on the uptake % of ^{137}Cs, ^{60}Co and $^{(152+154)}Eu$ from the radioactive liquid waste on fly ash at the ambient room temperature (25±1°C) and pH 8 .

Time, min	Uptake, %		
	Cs^{+}	Co^{2+}	Eu^{3+}
5	50.0	69.0	78.2
10	53.7	73.0	81.9
20	55.1	77.0	84.7
30	55.5	81.4	89.0
40	56.6	85.9	93.0
60	57.3	85.7	93.2
90	56.9	85.4	93.4
120	57.0	85.6	93.1
150	57.2	85.3	93.1
180	57.3	85.9	93.7
210	56.8	85.9	93.5

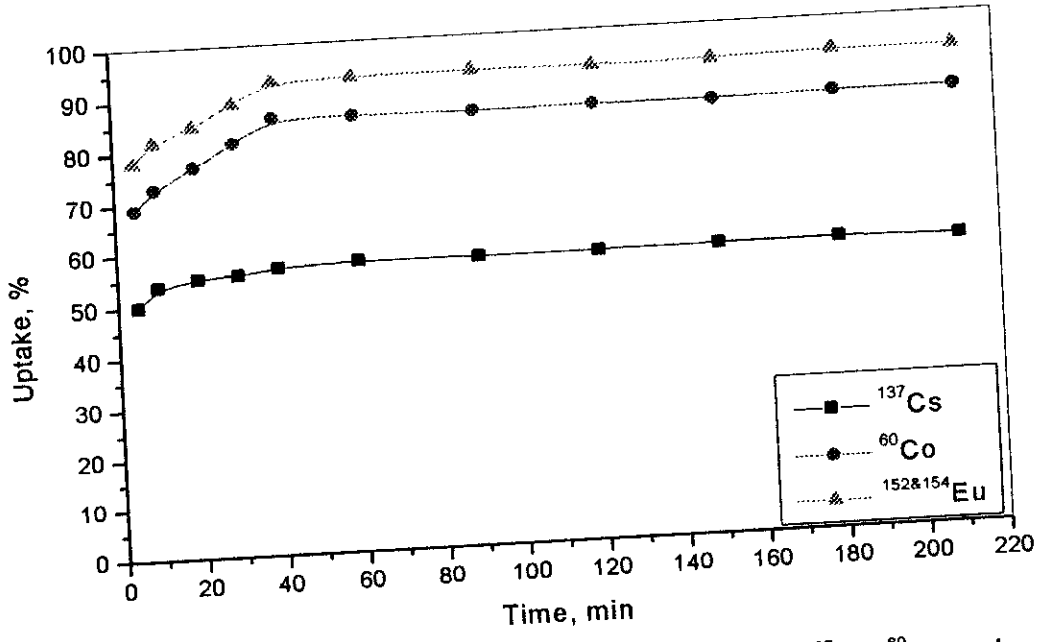

Fig. (8): Effect of shaking time on the uptake% of ^{137}Cs, ^{60}Co and $^{152,154}Eu$ from the radioactive liquid waste on fly ash.

Table (10): Effect of shaking time on the uptake % of ^{137}Cs, ^{60}Co and $^{(152+154)}Eu$ from the radioactive liquid waste on silica fume at the ambient room temperature (25±1°C) and pH 8 .

Time, min	Uptake, %		
	Cs^{+}	Co^{2+}	Eu^{3+}
5	52.0	70.2	81.2
10	58.3	77.1	84.5
20	60.7	83.4	86.8
30	61.3	87.5	89.9
40	63.3	90.8	93.2
60	65.8	90.9	93.3
90	65.8	90.7	93.3
120	65.7	91.1	93.1
150	65.8	91.1	93.4
180	65.3	91.2	93.3
210	65.8	91.3	93.3

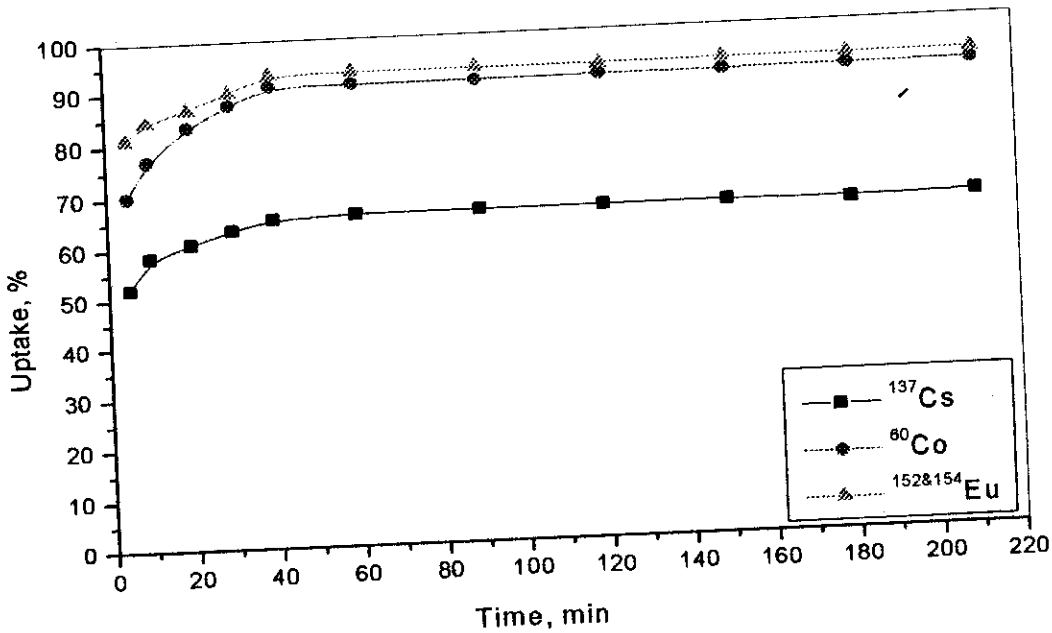

Fig. (9): Effect of shaking time on the uptake% of ^{137}Cs, ^{60}Co and $^{152,154}Eu$ from the radioactive liquid waste on silica fume.

Table (11): Effect of shaking time on the uptake % of ^{137}Cs, ^{60}Co and $^{(152+154)}Eu$ from the radioactive liquid waste on ceramic at the ambient room temperature (25±1°C) and pH 8 .

Time, min	Uptake, %		
	Cs^{+}	Co^{2+}	Eu^{3+}
5	56.0	72.0	82.3
10	62.3	78.0	84.2
20	66.1	84.0	89.2
30	67.6	88.7	92.8
40	68.8	91.2	96.9
60	69.1	91.1	97.1
90	69.4	91.3	97.4
120	69.4	91.1	97.3
150	69.4	91.2	97.2
180	69.4	91.0	97.2
210	69.4	91.0	97.1

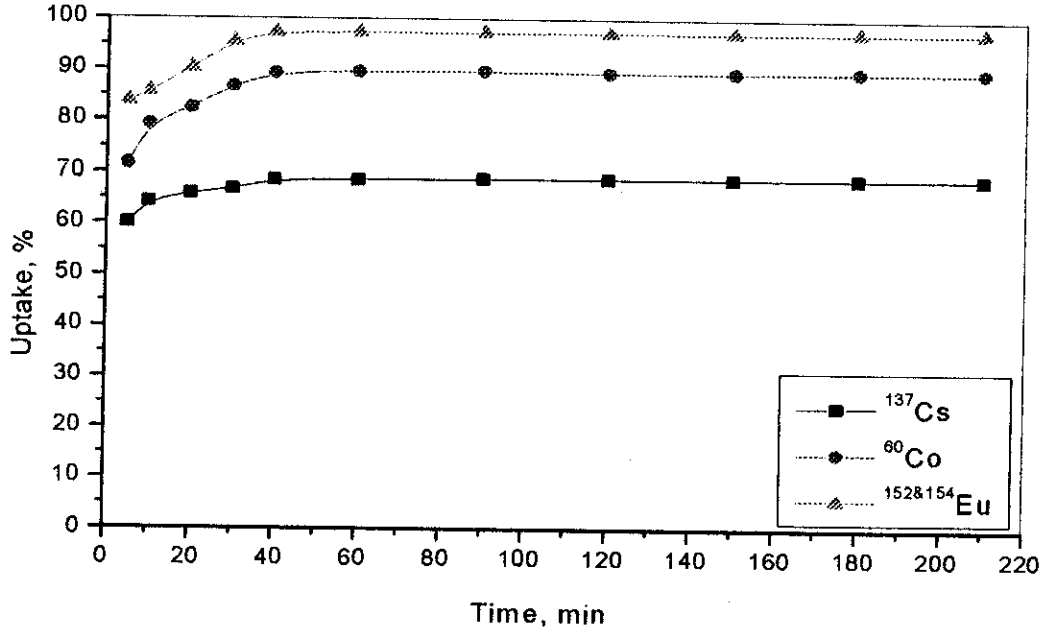

Fig. (11): Effect of shaking time on the uptake% of ^{137}Cs, ^{60}Co and $^{152,154}Eu$ from the radioactive liquid waste on window glass.

The uptake % at equilibrium (40 min.) for the radioactive liquid waste containing radioisotopes Cs-137, Co-60 and Eu(152+154) using the industrial solid wastes under investigation was given in Table (13).

Table (13): Uptake % at equilibrium (40 min) for the radioactive liquid waste containing Cs-137, Co-60, or Eu-(152+154) using the industrial solid wastes (homra, fly ash, silica fumes, ceramic and window glass).

Industrial Materials	uptake % at equilibrium		
	Cs^{+}	Co^{2+}	Eu^{3+}
Homra	92.9	94.1	98.9
Fly ash	56.6	85.9	93.0
Silica fumes	65.3	90.8	93.2
Ceramic	68.8	91.2	96.9
Window glass	68.7	89.3	97.3

Data show that, homra has the highest uptake rather than the other solids. Fly ash shows low uptake values which may be attributed to its finest particle size **(Vagelis 2000)** so the ions are large enough that they can not fill the micro pores on its surface.

For all industrial solids used, the uptake % values were arranged according to the sequence:

Homra > ceramic = window glass > silica fume > fly ash.

4.3. Decontamination factor:

Decontamination factor (DF) that assesses the efficiency for the removal of the investigated radionuclides Cs^{+}, Co^{2+} and Eu^{3+} from the bulk of liquid waste solution using the industrial solid wastes: homra, fly ash, silica fume, ceramic and window glass was calculated and the results are listed in Table (14).

Table (14): Decontamination factor values for cesium-137, cobalt-60 and europium-(152+154) on the sorbent materials used.

Sorbent materials	Decontamination factor, DF		
	Cs^{+}	Co^{2+}	Eu^{3+}
Homra	14.0	17.1	93.0
Fly ash	2.3	7.1	14.4
Silica fume	2.9	10.9	14.6
Ceramic	3.2	11.4	33.1
Window glass	3.2	9.4	36.7

From this table it can be concluded that DF shows its greatest value with homra (homra has great efficiency) for the removal of the investigated radioactive cations as it shows the highest uptake values.

4.4. Effect of pH:

The effect of pH (2-11) on the uptake % of ^{137}Cs, ^{60}Co and $^{152+154}Eu$ with particle size 0.1mm of the industrial solid wastes: homra, fly ash, silica fume, ceramic and window glass as sorbents, was evaluated at the ambient room temperature (25±1°C) and shaking time of one hour. The obtained results are presented in Tables (15-19).

From these tables it can be concluded that, the uptake of the investigated radioisotopes is inhibited in the acidic medium, pH ≤ 2 after which the sorption increases sharply with the increase in the pH of the aqueous solution to attain maximum values around the alkaline medium (pH 8 and higher). The variation observed in the results is explained on the basis of the fact that the metal oxide surfaces in the aqueous solution carry a surface charge which is dependent on the zero point charge of the oxide as well as on the pH of the solution. Such a pH-dependent charge is developed by protonation and deprotonation reactions with oxo, hydroxo and aquo ligands present in the bulk solution **(Park 1967)**. The sorption in acidic region is found relatively less, which is due to the competition between the excess of H^+ in the medium and the positively charged examined species Cs^+, Co^{2+} and Eu^{3+} present in the aqueous solution **(Ezz El-Din et al 2001)** .

Also from Figs (12-16) it can be deduced that, at higher pH values the uptake of Cs-137 and Eu-(152+ 154) decreased once more (i.e. desorbed), which may be attributed to the formation of hydrolyzed Cs^+ and Eu^{3+} species in the solution but Co^{2+} increased with increasing pH **(Abdelraouf M.W et al 1997)**.The uptake for the studied radioisotopes was found in the order of their cationic charge, i.e. $Eu^{3+} > Co^{2+} > Cs^+$.

Table (15): Effect of pH on the uptake % of ^{137}Cs, ^{60}Co and $^{(152+154)}Eu$ from the radioactive liquid waste on homra at the ambient room temperature (25±1°C) and shaking time of one hour.

PH	Uptake, %		
	Cs^{+}	Co^{2+}	Eu^{3+}
2	43.0	26.3	63.7
3	56.2	32.1	72.2
4	65.1	38.3	81.9
5	70.8	48.0	86.4
6	78.7	69.7	89.6
7	86.0	84.7	96.3
8	92.8	93.8	98.2
9	79.4	94.7	98.7
10	73.3	95.2	99.5
11	65.0	95.9	72.8

Table (16): Effect of pH on the uptake % of ^{137}Cs, ^{60}Co and $^{(152+154)}Eu$ from the radioactive liquid waste on fly ash at the ambient room temperature (25±1°C) and shaking time of one hour.

PH	Uptake, %		
	Cs^{+}	Co^{2+}	Eu^{3+}
2	12.0	21.4	45.8
3	21.9	33.2	63.7
4	32.2	43.2	82.1
5	40.6	54.2	87.3
6	46.7	66.3	89.6
7	52.2	78.1	90.6
8	55.9	86.2	92.8
9	51.9	86.8	95.7
10	34.2	87.2	98.2
11	25.1	87.9	62.1

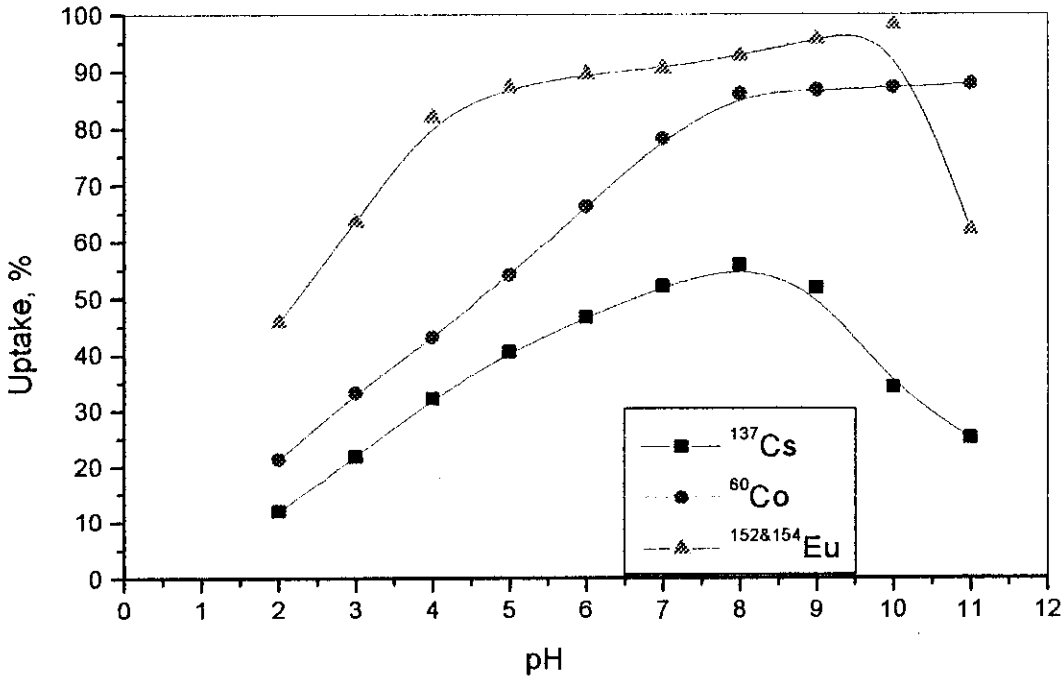

Fig. (13): Effect of pH on the uptake % of ^{137}Cs, ^{60}Co and $^{152\&154}Eu$ from the radioactive liquid waste on fly ash.

Table (17): Effect of pH on the uptake % of ^{137}Cs, ^{60}Co and $^{(152+154)}Eu$ from the radioactive liquid waste on silica fume at the ambient room temperature (25±1°C) and shaking time of one hour.

PH	Uptake, %		
	Cs^{+}	Co^{2+}	Eu^{3+}
2	13.0	17.3	26.3
3	28.0	33.3	43.9
4	36.0	46.9	78.1
5	44.1	59.2	84.3
6	52.2	72.1	88.4
7	58.0	83.9	90.3
8	64.6	92.1	92.6
9	53.0	94.6	96.3
10	47.0	96.2	98.0
11	34.0	98.4	60.9

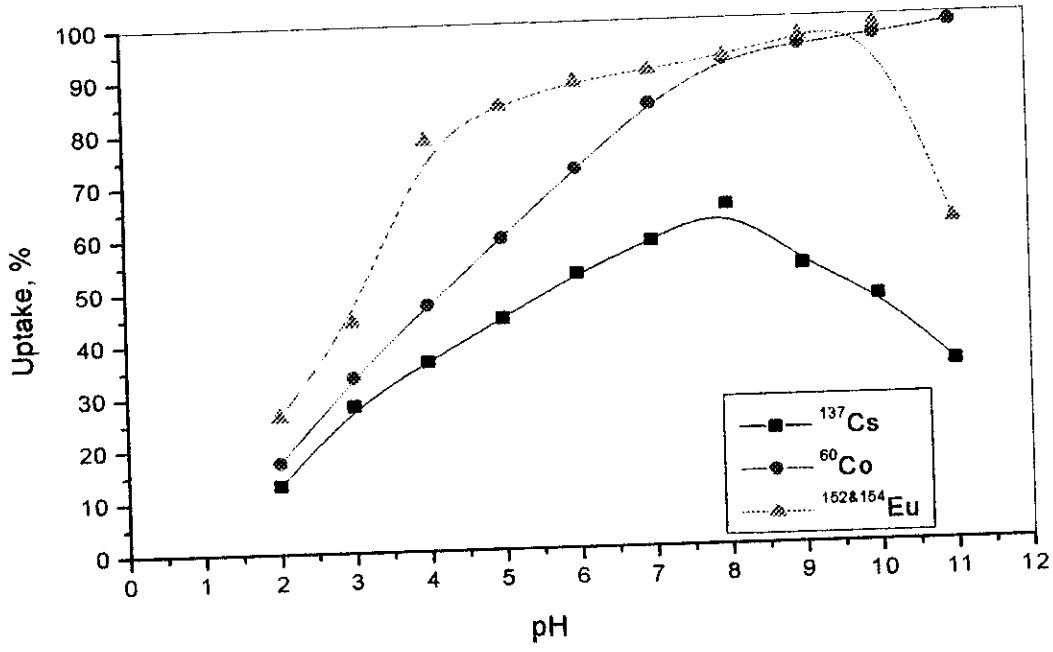

Fig. (14): Effect of pH on the uptake % of ^{137}Cs, ^{60}Co and $^{152\&154}Eu$ from the radioactive liquid waste on silica fume.

Table (18): Effect of pH on the uptake % of ^{137}Cs, ^{60}Co and $^{(152+154)}Eu$ from the radioactive liquid waste on ceramic at the ambient room temperature (25±1°C) and shaking time of one hour.

PH	Uptake, %		
	Cs^{+}	Co^{2+}	Eu^{3+}
2	1.9	12.3	54.3
3	14.1	26.4	62.7
4	30.7	36.3	73.1
5	42.3	47.5	79.9
6	53.6	59.7	86.4
7	61.2	74.3	94.1
8	68.6	90.8	96.8
9	56.7	92.1	97.2
10	39.6	93.7	97.6
11	32.5	94.4	66.3

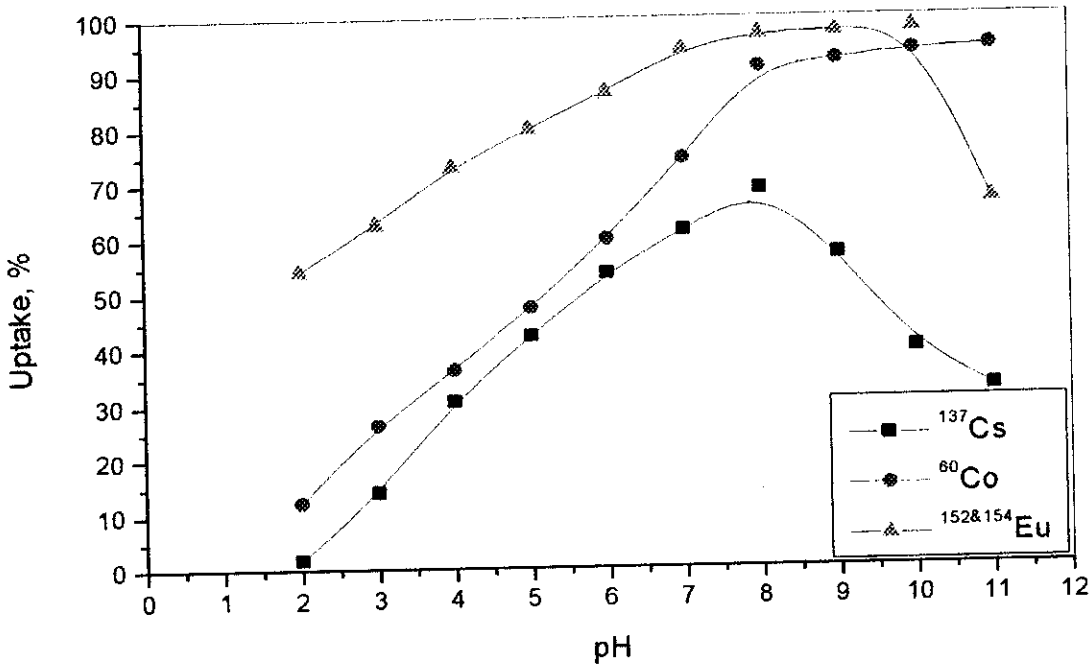

Fig. (15): Effect of pH on the uptake % of ^{137}Cs, ^{60}Co and $^{152\&154}Eu$ from the radioactive liquid waste on ceramic.

Table (19): Effect of pH on the uptake % of ^{137}Cs, ^{60}Co and $^{(152+154)}Eu$ from the radioactive liquid waste on window glass at the ambient room temperature (25±1°C) and shaking time of one hour.

PH	Uptake, %		
	Cs^{+}	Co^{2+}	Eu^{3+}
2	2.9	8.1	35.9
3	16.6	29.9	53.2
4	30.1	42.3	71.2
5	42.0	54.1	79.5
6	49.9	65.2	88.3
7	59.9	76.4	93.7
8	67.2	88.8	97.4
9	53.2	90.1	97.9
10	45.6	91.4	98.1
11	29.1	91.9	64.2

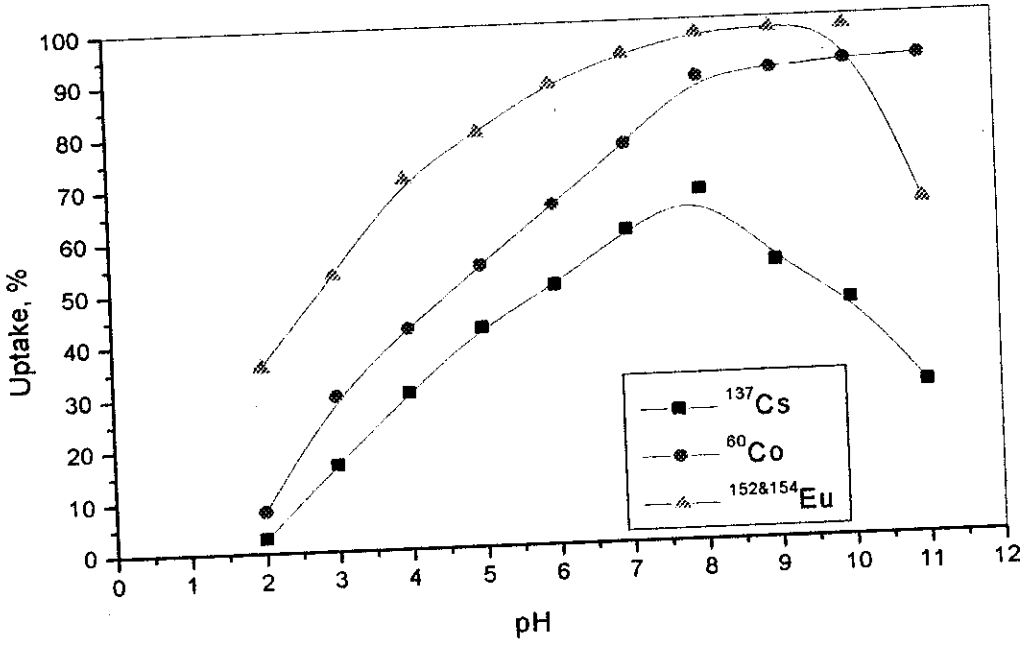

Fig. (16): Effect of pH on the uptake% of ^{137}Cs, ^{60}Co and $^{152\&154}Eu$ from the radioactive liquid waste on window glass.

4.5. Effect of liquid/solid ratio:

The effect of sorbent weight to volume of the radioactive liquid waste on the uptake was evaluated with 0.1mm of the industrial solid wastes; homra, fly ash, silica fumes, ceramic and window glass at the ambient room temperature (25±1°C), shaking time of one hour and pH 8. The obtained results are listed in Tables (20-24) which show, as it was accepted, increasing in the weight of sorbent increases the uptake. This can be explained as, increasing the sorbent amount increases the active sites which increases the ions that occupy these sites .

This behavior was observed with cesium and cobalt and not observed with europium, where there is no effect with increasing solid weight on the uptake of europium. This may be attributed to its smallest ion size that can occupy all kinds of pores, $Eu^{3+} < Co^{2+} < Cs^{+}$.

Table (20): Effect of industrial solid waste weight of homra on the uptake of ^{137}Cs, ^{60}Co and $^{152+154}Eu$ from low level liquid waste at the ambient room temperature (25±1°C), pH 8 and shaking time of one hour.

Solid wt, g	Uptake, %		
	Cs^{+}	Co^{2+}	Eu^{3+}
0.05	74.6	83.6	97.7
0.10	79.0	87.5	98.2
0.15	83.0	91.1	98.3
0.20	91.7	93.7	97.9
0.25	94.6	96.2	98.4

Table (21): Effect of industrial solid waste weight of fly ash on the uptake of ^{137}Cs, ^{60}Co and $^{152+154}Eu$ from low level liquid waste at the ambient room temperature (25±1°C), pH 8 and shaking time of one hour.

Solid wt, g	Uptake, %		
	Cs^{+}	Co^{2+}	Eu^{3+}
0.05	19.7	77.3	88.9
0.10	32.7	81.2	89.8
0.15	41.4	83.7	90.1
0.20	54.2	86.4	92.8
0.25	58.3	89.2	93.9

Table (22): Effect of industrial solid waste weight of silica fume on the uptake of ^{137}Cs, ^{60}Co and $^{152+154}Eu$ from low level liquid waste at the ambient room temperature (25±1°C), pH 8 and shaking time of one hour.

Solid wt, g	Uptake, %		
	Cs^{+}	Co^{2+}	Eu^{3+}
0.05	18.2	76.9	92.1
0.10	25.3	81.9	92.6
0.15	30.0	86.2	92.9
0.20	63.9	91.2	93.7
0.25	66.3	94.8	94.4

Table (23): Effect of industrial solid waste weight of ceramic on the uptake of ^{137}Cs, ^{60}Co and $^{152+154}Eu$ from low level liquid waste at the ambient room temperature (25±1°C), pH 8 and shaking time of one hour.

Solid wt, g	Uptake, %		
	Cs^{+}	Co^{2+}	Eu^{3+}
0.05	28.3	86.7	96.2
0.10	35.8	88.1	96.8
0.15	40.3	89.6	97.5
0.20	68.8	91.2	97.3
0.25	74.6	95.4	98.2

Table (24): Effect of industrial solid waste weight of window glass on the uptake of ^{137}Cs, ^{60}Co and $^{152+154}Eu$ from low level liquid waste at the ambient room temperature (25±1°C), pH 8 and shaking time of one hour.

Solid wt, g	Uptake, %		
	Cs^{+}	Co^{2+}	Eu^{3+}
0.05	24.2	79.6	94.1
0.10	39.8	82.1	94.3
0.15	52.8	84.6	95.1
0.20	67.6	89.2	96.4
0.25	72.2	94.3	96.9

4.7. Effect of particle size :

The variation of sorbents particle size (0.07, 0.08, 0.1, 0.15, 0.2, 0.25 mm) with the sorption percent of the radioactive ions ^{137}Cs, ^{60}Co and $^{152+154}Eu$ using the industrial solid wastes: homra, fly ash, silica fume, ceramic and window glass at the ambient room temperature (25±1°C), pH8 and shaking time of one hour was investigated and the results obtained are given in Tables (25-29)

From these tables it was found that, all solids give very small change (almost no change) in the uptake of the radioactive ions with different particle size **(Ognyan 1995)** except window glass which shows the greatest difference in sorption as the particle size changes, this may be attributed to its small surface area.

Table (25): The effect of particle size of industrial solid waste homra on the uptake % of ^{137}Cs, ^{60}Co or $^{152+154}Eu$ from low level radioactive waste at the ambient room temperature (25±1°C), pH 8 and shaking time of one hour.

Particle size, mm	Uptake, %		
	Cs^{+}	Co^{2+}	Eu^{3+}
0.07	89.3	90.7	96.2
0.08	90.2	92.6	96.9
0.10	91.3	93.7	98.2
0.15	92.2	94.1	98.7
0.20	92.7	95.3	99.2
0.25	93.2	95.9	99.7

Table (26): Effect of particle size of industrial solid waste fly ash on the uptake % of ^{137}Cs, ^{60}Co or $^{152+154}Eu$ from low level radioactive waste at the ambient room temperature (25±1°C), pH 8 and shaking time of one hour.

Particle size, mm	Uptake, %		
	Cs^{+}	Co^{2+}	Eu^{3+}
0.07	53.3	85.1	91.2
0.08	54.8	85.6	92.1
0.10	56.2	86.3	92.7
0.15	57.4	86.7	93.1
0.20	57.9	87.3	94.3
0.25	58.3	88.0	95.2

Table (27): Effect of particle size of industrial solid waste silica fume on the uptake % of ^{137}Cs, ^{60}Co or $^{152+154}Eu$ from low level radioactive waste at the ambient room temperature (25±1°C), pH 8 and shaking time of one hour.

Particle size, mm	Uptake, %		
	Cs^{+}	Co^{2+}	Eu^{3+}
0.07	62.6	87.7	91.7
0.08	63.2	89.1	92.8
0.10	64.7	90.6	93.4
0.15	65.2	91.2	94.7
0.20	66.7	92.6	96.3
0.25	67.1	93.5	98.1

Table (28): Effect of particle size of industrial solid waste ceramic on the uptake % of ^{137}Cs, ^{60}Co or $^{152+154}Eu$ from low level radioactive waste at the ambient room temperature (25±1°C), pH 8 and shaking time of one hour.

Particle size, mm	Uptake, %		
	Cs^{+}	Co^{2+}	Eu^{3+}
0.07	66.1	88.3	94.3
0.08	66.8	89.7	95.6
0.10	68.1	90.6	96.8
0.15	69.3	91.0	97.1
0.20	70.3	92.2	97.6
0.25	70.9	92.7	98.2

Table (29): Effect of particle size of industrial solid waste window glass on the uptake % of ^{137}Cs, ^{60}Co or $^{152+154}Eu$ from low level radioactive waste at the ambient room temperature (25±1°C), pH 8 and shaking time of one hour.

Particle size, mm	Uptake, %		
	Cs^{+}	Co^{2+}	Eu^{3+}
0.07	61.2	82.2	86.2
0.08	64.1	86.4	92.8
0.10	67.9	90.1	97.1
0.15	69.1	92.0	98.2
0.20	72.7	95.3	98.7
0.25	74.6	96.7	99.1

4.7. Properties of the Immobilized Waste Forms:

In this section the effect of the industrial solid waste materials (homra, fly ash, silica fume, ceramic and window glass) on the ordinary portland cement properties when mixed with them was evaluated. Many factors were studied in this respect curing time, initial and final setting times, bleeding test, mechanical strength, water immersion and leachability (rapid and long term testes).

4.7.1. Effect of curing time:

The effect of curing time on the mechanical strength of plain ordinary portland cement and ordinary portland cement mixed with the industrial solid wastes: homra, fly ash, silica fume ceramic and window glass with water / cement ratio of 0.35 after curing time 7, 14, 21, 28, and 60 days was evaluated and the results obtained are presented in Table (30) and graphically in Fig (17).

From these data it can be conclude that, the mechanical strength for all the cement samples mixed with the industrial solids increases with increasing the curing period. The maximum mechanical strength value was obtained after curing for 28 days and after that it almost remains constant **(Raafat and Pat 1986)**.

Table (30): Effect of curing time on the mechanical strength of plain ordinary portland cement and cement mixed with homra, fly ash, silica fume ceramic and window glass.

Composition	Mechanical strength kg /cm^2				
	7 days	14days	21 days	28 days	60 days
Plain OPC	23.3	30.2	41.3	48.1	48.9
OPC + homra	34.2	46.1	55.9	66.7	67.1
OPC+ fly ash	29.1	38.6	46.6	57.4	57.9
OPC+ silica fume	37.9	49.8	59.8	70.9	71.4
OPC + ceramic	30.1	43.4	50.6	61.9	62.2
OPC + window glass	26.3	37.5	43.8	51.9	52.3

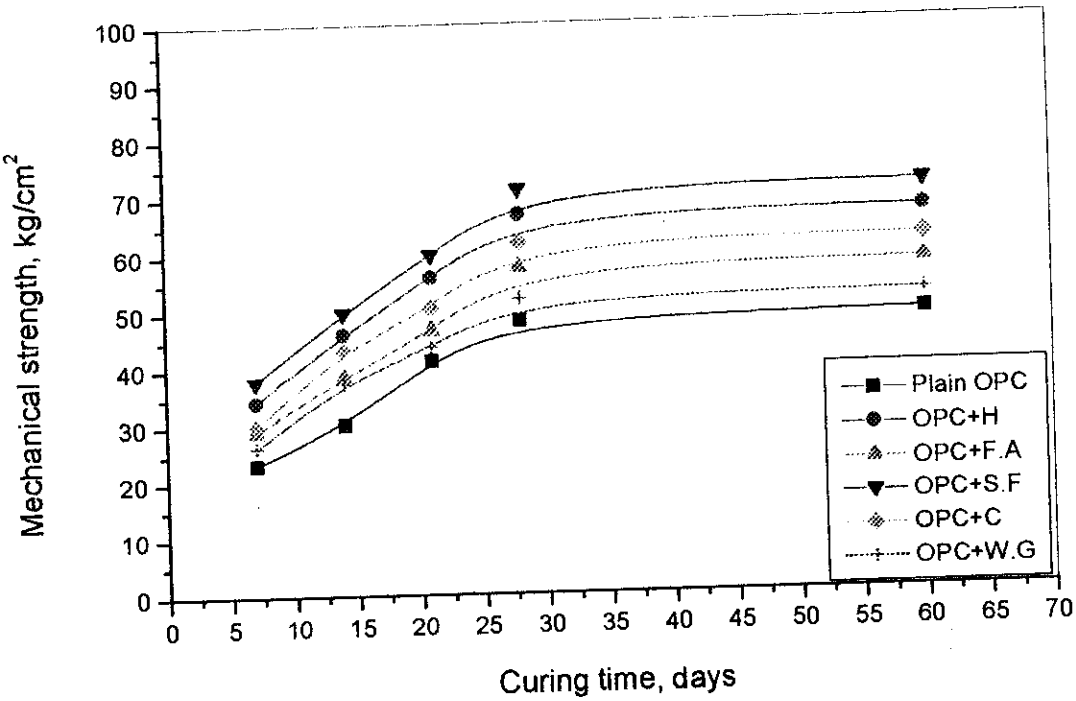

Fig. (17): Mechanical strength as a function of curing time for cement and cement mixed with the industrial solid wastes.

4.7.3 Bleeding investigations:

The bleeding capacity (%) and bleeding rate (ml / h) of the cement pastes (plain ordinary portland cement (OPC), OPC mixed with homra, OPC mixed with fly ash, OPC mixed with silica fume, OPC mixed with ceramic and OPC mixed with window glass) with a solid / cement ratio of 5% and a water/cement ratio of 0.35 were investigated and results obtained are given in Table (32).

From this table it can be concluded that, in general all the solids added to cement pastes decrease the bleeding capacity and the bleeding rate . This may be attributed to that when the solids are added to the cement they are adsorbed on its surface and produce a pore structure more discontinuous and impermeable than that of the cement paste alone, as a result the pores are closed and the bleeding is inhibited.

Also the cement mixed with fly ash, shows the lowest values of bleeding capacity and bleeding rate , this may be attributed to its great fineness.

For all industrial solids added , the bleeding of the cement pastes are arranged according to the following sequence

fly ash < silica fume < window glass < ceramic < homra < plain OPC.

Table (32): The Bleeding capacity (%) and Bleeding rate (ml/h) of plain ordinary portland cement and cement mixed with the industrial solid wastes (homra, fly ash, silica fume, ceramic and window glass).

Composition	Bleeding Capacity, (%)	Bleeding rate, (ml / h)
Plain OPC	3.8	2.0E-2
OPC + homra	3.2	1.6E-2
OPC + fly ash	1.3	0.7E-2
OPC + silica fume	1.6	0.8E-2
OPC + ceramic	2.9	1.5E-2
OPC + window glass	2.2	1.1E-2

4.7.4. Mechanical strength investigations:

The mechanical strength development of plain ordinary portland cement and ordinary portland cement mixed with industrial solid wastes: homra, fly ash, silica fume, ceramic and window glass at different weight percents; 5, 10, 15, 20, 25, and 30 homra, flay ash, silica fume, ceramic and window glass was tested and the results obtained are listed in Table (33).

From this table, it can be conclude that, the mechanical strength increases with the addition of homra lower to15% then it decreases. The higher mechanical strength of the cement pastes with 5, 10 and 15 wt. % homra replacement than the controlled one (no solid replacement) is due to the pozzolanic reaction of homra with the liberated lime to produce additional amount of calcium silicate hydrate (CSH) and aluminosilicate hydrate. The decrease of the mechanical strength of 20, 25 and 30 wt % homra replacement, is due to the decrease of the clinker content **(Heikal and El-Didamony 1999)**.

The 15 wt % replacement of homra improves the mechanical strength by 18.5% more than the control one (plain OPC).

Ceramic replacement shows the same behavior of homra, since they almost have the same silica percent and the same active groups.

Generally, when portland cement is replaced by fly ash, the final strength exceeds that of the controlled one only if the content of the active silica in the fly ash is higher than that in the cement **(Zhang et al 1997)**

Table (33): The mechanical strength of plain ordinary portland cement and cement mixed with different weight percents of the industrial solid wastes (homra, fly ash, silica fume, ceramic and window glass) cured at 28 days.

Composition	Mechanical strength, kg/cm^2						
	Plain	5%	10%	15%	20%	25%	30%
OPC+homra	50.2	67.9	74.1	79.3	69.2	62.5	56.2
OPC+fly ash	50.2	58.4	53.4	50.1	47.3	45.2	41.4
OPC+silica fume	50.2	70.1	76.3	81.9	67.6	62.1	58.2
OPC+ceramic	50.2	61.2	67.8	74.9	59.1	55.3	48.1
OPC+window glass	50.2	50.9	53.4	59.1	62.3	56.4	52.1

Although fly ash contains the lowest percent of silica but it has high percent of the active groups.

When cement is replaced by silica fume, the strengths become much higher than the controlled one, i.e. silica fume shows a superior performance **(Chandra and Berntsson 1997)** when added to the cement paste, (Fig 18). This can be attributed to the content of silica in silica fume (about 95%) is much higher than that of cement (about 19%) and such a replacement leads to higher CSH-content (provided enough CH is available). When the CH is completely consumed, additional replacement will lead to decrease of strength **(Papadaskis 1999).**

Also from Fig (18) it is found that window glass-cement mixture has the lower strengths than others at the age of 28 days at the ambient room temperature (25±1°C) this can be attributed to the relatively low percentage of the active components, (SiO_2+ Al_2O_3+Fe_2O_3) in window glass **(Yixin et al 2000)**, Table (7). This makes window glass less reactive.

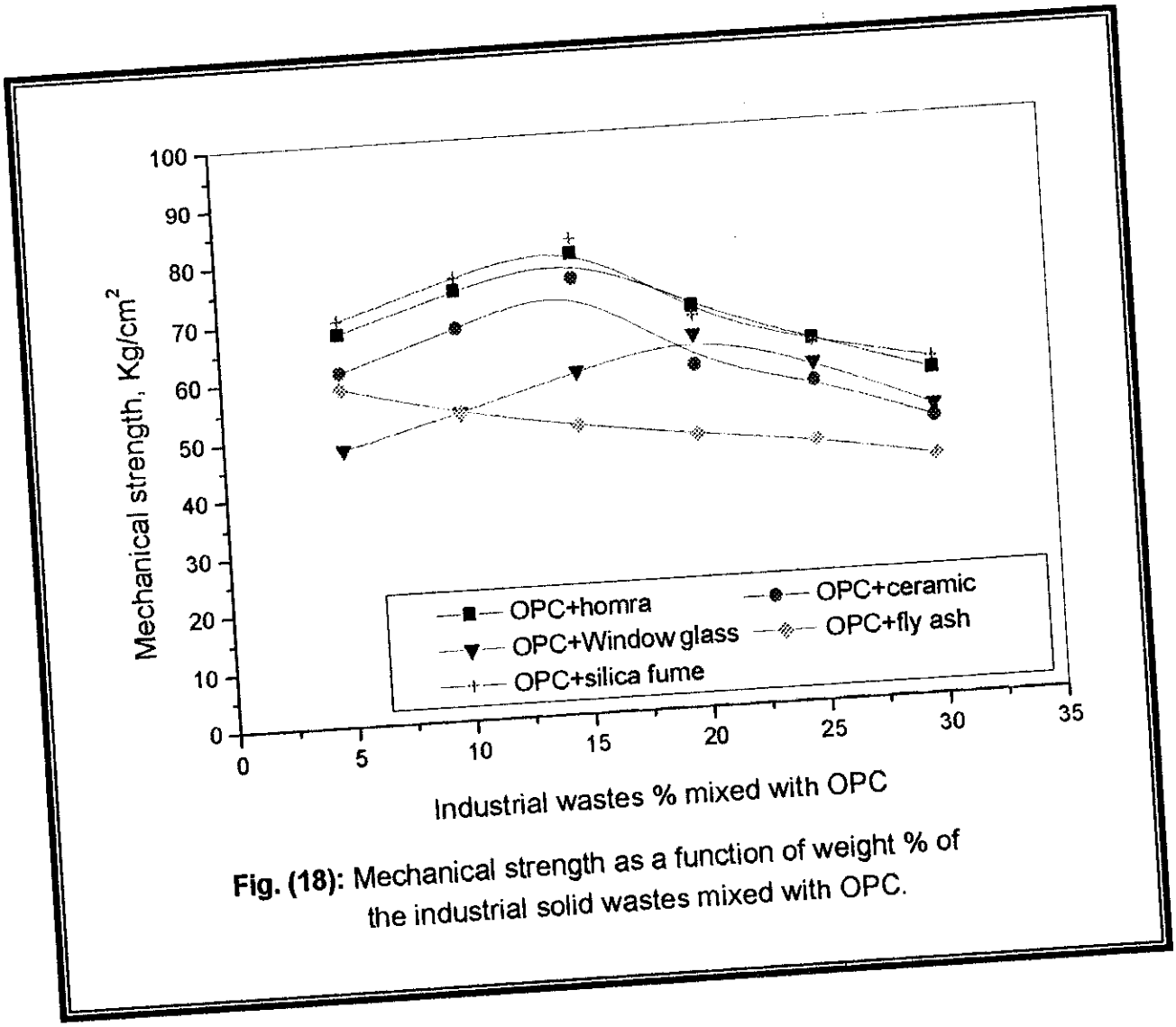

Fig. (18): Mechanical strength as a function of weight % of the industrial solid wastes mixed with OPC.

4.7.5. Effect of water immersion:

The effect of water immersion on the mechanical strength of plain ordinary portland cement and cement mixed with the industrial solid wastes homra, fly ash, silica fume, ceramic and window glass pastes were examined and the results obtained are given in Table (34) . The samples were immersed in sea water, tap water and distilled water for one and three months.

The data indicated that, ordinary portland cement mixed with industrial solid wastes has higher mechanical strength than that without any additives, which is attributed to pozzolanic reactions **(Heikal and El-Didamony 1999)**. Also the mechanical strength increased as the time period of immersion increased from one to three months.

Samples immersed in sea water have mechanical strength values higher than that immersed in tap water or distilled water . This is due to that, the immersing medium (sea water) acts as an accelarator and the sulfate ions activate the hydration of the cement pastes **(El-Didamony et al 1996)**. As a result of this activation, calcium sulphoaluminate and calcium silicate hydrates are formed filling up the available pore volume and leading to increasing in mechanical strength. The mechanical strength of cement samples immersed in sea water can be arranged according to the following sequence:

(OPC+W.G) > (OPC+S.F) > (OPC+F.A) > (OPC+C) > (OPC+H) > plain OPC.

Also it was concluded that, the effect of immersing medium on the mechanical strength of cement samples after immersion in different types of water for one and three months have the following sequence:

sea water > distilled water > tap water.

Table (34): Effect of water immersion on the mechanical strength of plain ordinary portland cement and cement mixed with the industrial solid wastes: homra, fly ash, silica fume, ceramic and window glass in sea water, tap water and distilled water for one and three months .

Composition	Mechanical strength, kg/cm^2					
	Sea water		Tap water		Distilled water	
	One month	Three months	One month	Three months	One month	Three months
Plain OPC	49.6	52.1	46.9	48.9	48.2	50.9
OPC+homra	50.2	55.3	49.2	51.2	49.8	52.7
OPC+fly ash	57.8	62.1	56.8	58.1	57.3	59.8
OPC+silica fume	60.1	66.3	58.1	60.9	58.5	62.2
OPC+ceramic	52.9	56.6	51.7	53.2	52.1	55.2
OPC+window glass	64.8	69.2	61.9	65.4	63.7	67.9

4.7.6. Leachability investigations:

Leachability is the measure of radionuclides transported to environment by an aqueous medium. The development of processes for immobilizing radioactive liquid wastes adsorbed on industrial solid wastes homra, fly ash, silica fume, ceramic and window glass mixed with ordinary portland cement to give a solid product limits the mobility of radioactive nuclides to a safe and cheap storage of the waste. In order to take full advantage of such possibility, it is necessary to determine the characteristics of leaching radioactive materials from the solidified waste forms.

4.7.6.1 Long-term leachability:

The cumulative fractions of Cs^{+}, Co^{2+} and Eu^{3+} leached from the solidified waste forms containing plain OPC and OPC mixed with homra, fly ash, silica fume, ceramic or window glass immersed in deionized water for 1, 2, 3, 4, 5, 6, 7, 14, 21, 28, 35, 65 and 95 day were studied and the results obtained are presented in Tables (35-37).

From the listed data, it can be concluded that, the rate of the cumulative fractions for all samples decrease with increasing the immersion time because of decreasing the rate of calcium hydroxide formation.

The cumulative fractions of the solidified waste forms mixed with homra, fly ash, silica fume, ceramic or window glass contaminated with Cs^{137}, Co^{60}, or $Eu^{152+154}$ are arranged according to the following sequence:
OPC > (OPC+S.F) > (OPC+F.A) > (OPC+C) > (OPC+H) > (OPC+W.G).

For all investigated radioactive ions, the leaching rate can be arranged according to the following sequence: $Cs^{+} > Co^{2+} > Eu^{3+}$ **(Shen et al 1993)**.

The obtained results are also presented in Figs (19-21), from which it can be concluded that, the solidified waste forms with all industrial solid waste additives have lower cumulative fractions than that without additives and OPC alone has a maximum cumulative fraction. This may be attributed to that all solids added (pozzolanic materials) contain silica and alumina which react with calcium hydroxide (lime) produced during the hydration of cement to form calcium silicates which prevent the movement and diffusion of the radionuclides from the immobilized waste **(Takemoto and Uchikawa 1986)**.

Also cement paste mixed with window glass has an excellent leach resistance property (has the lowest cumulative fraction) **(International Atomic Energy Agency 2002).**

Table (35): Cumulative fractions of cesium-137 leached from the solidified waste forms immersed in distilled water as a function of leaching times at the ambient room temperature (25 ± 1°C).

Time (day)	Cumulative fraction, cm					
	Plain OPC	OPC + H	OPC + F.A	OPC + S.F	OPC + C	OPC + W.G
1	9.8E-4	5.2E-4	7.1E-4	8.3E-4	6.8E-4	3.1E-4
2	3.3E-3	8.1E-4	9.6E-4	1.3E-3	9.4E-4	6.7E-4
3	7.9E-3	1.6E-3	3.9E-3	5.2E-3	2.7E-3	9.3E-4
4	1.4E-2	2.9E-3	5.7E-3	7.3E-3	5.2E-3	3.5E-3
5	2.6E-2	4.2E-3	8.2E-3	8.2E-3	7.8E-3	4.1E-3
6	3.1E-2	6.1E-3	1.1E-2	1.1E-2	9.3E-3	5.2E-3
7	3.6E-2	7.2E-3	1.5E-2	2.4E-2	1.1E-2	6.1E-3
14	3.9E-2	1.1E-2	2.2E-2	2.9E-2	1.9E-2	7.4E-3
21	4.3E-2	1.5E-2	2.5E-2	3.3E-2	2.3E-2	8.3E-3
28	4.7E-2	1.8E-2	3.1E-2	3.6E-2	2.6E-2	9.6E-3
35	5.1E-2	2.2E-2	3.6E-2	4.3E-2	2.9E-2	1.1E-2
65	6.2E-2	2.6E-2	3.9E-2	4.7E-2	3.3E-2	1.4E-2
95	6.6E-2	2.9E-2	4.2E-2	5.1E-2	3.5E-2	1.7E-2

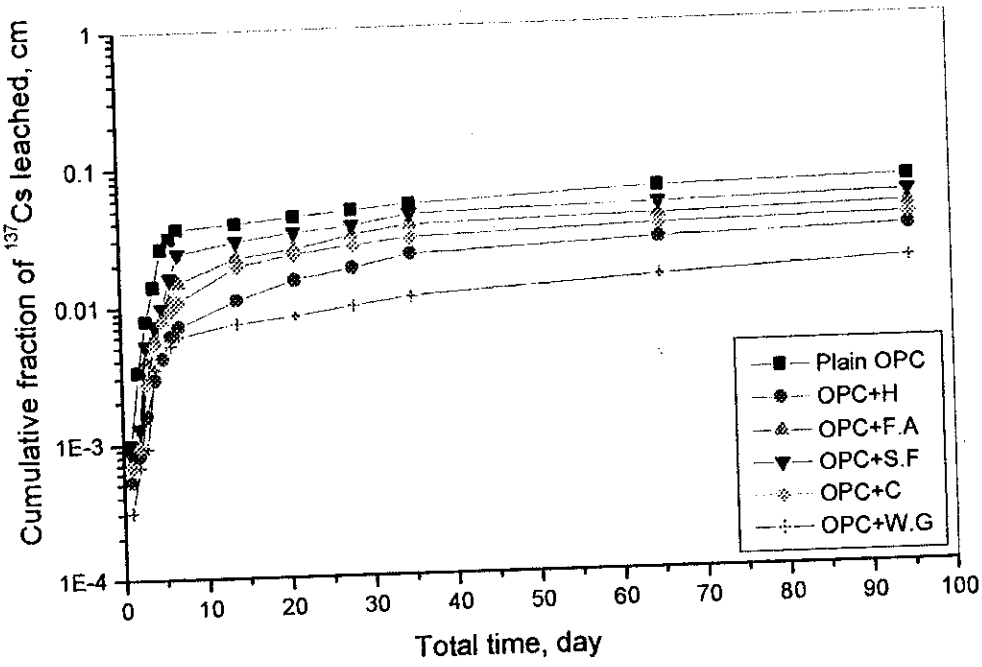

Fig.(19): variation of the cumulative fraction of ^{137}Cs leached from the solidified waste sample mixed with plain portland cement and portland cement mixed with the industrial solid materials as a function of the total leaching time.

Table (36): Cumulative fractions of cobalt-60 leached from the solidified waste forms immersed in distilled water as a function of leaching times at the ambient room temperature (25 ± 1°C).

Time (day)	Cumulative fraction, cm					
	Plain OPC	OPC + H	OPC + F.A	OPC + S.F	OPC + C	OPC + W.G
1	9.2E-4	2.8E-4	5.9E-4	7.2E-4	3.6E-4	1.8E-4
2	1.4E-3	6.3E-4	8.7E-4	9.4E-4	5.7E-4	3.9E-4
3	2.7E-3	8.9E-4	1.5E-3	1.9E-3	8.9E-4	5.1E-4
4	3.5E-3	1.2E-3	2.2E-3	2.7E-3	1.2E-3	7.6E-4
5	4.1E-3	1.5E-3	2.9E-3	3.6E-3	1.9E-3	9.8E-4
6	5.5E-3	1.8E-3	3.7E-3	4.5E-3	2.6E-3	1.3E-3
7	6.7E-3	2.2E-3	4.8E-3	5.1E-3	3.3E-3	1.6E-3
14	8.4E-3	2.9E-3	5.7E-3	6.2E-3	4.1E-3	2.0E-3
21	1.1E-2	3.8E-3	6.9E-3	8.1E-3	5.0E-3	2.5E-3
28	1.4E-2	4.7E-3	7.5E-3	9.2E-3	6.1E-3	3.0E-3
35	1.6E-2	5.2E-3	8.4E-3	1.1E-2	7.2E-3	3.4E-3
65	1.9E-2	5.7E-3	9.1E-3	1.3E-2	7.6E-3	3.9E-3
95	2.1E-2	6.1E-3	9.7E-3	1.4E-2	8.2E-3	4.4E-3

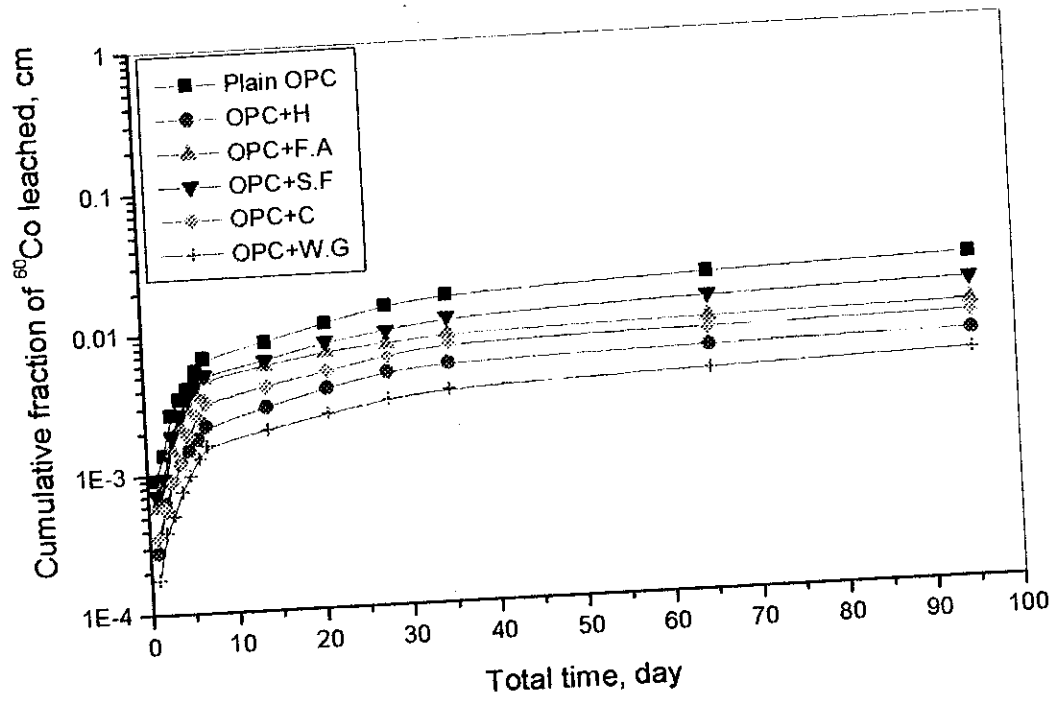

Fig. (20): variation of the cumulative fraction of ^{60}Co leached from the solidified waste sample mixed with plain portland cement and portland cement mixed with the industrial solid materials a function of the total leaching time.

Table (37): Cumulative fractions of europium-(152+154) leached from the solidified waste forms immersed in distilled water as a function of leaching times at the ambient room temperature (25 ± 1°C).

Time (day)	Cumulative fraction, cm					
	Plain OPC	OPC + H	OPC + F.A	OPC + S.F	OPC + C	OPC + W.G
1	4.2E-4	1.7E-4	2.7E-4	3.4E-4	2.2E-4	1.3E-4
2	7.6E-4	2.2E-4	4.6E-4	5.1E-4	3.7E-4	2.1E-4
3	1.1E-3	4.3E-4	6.2E-4	6.9E-4	4.5E-4	2.9E-4
4	1.5E-3	5.6E-4	7.8E-4	8.1E-4	6.2E-4	3.7E-4
5	1.9E-3	6.3E-4	8.6E-4	9.8E-4	7.1E-4	4.2E-4
6	2.2E-3	7.1E-4	9.7E-4	1.2E-3	8.4E-4	4.9E-4
7	2.6E-3	8.2E-4	1.2E-3	1.6E-3	9.6E-4	5.3E-4
14	3.2E-3	1.1E-3	1.7E-3	2.3E-3	1.5E-3	7.5E-4
21	3.6E-3	1.4E-3	2.1E-3	2.8E-3	1.8E-3	9.6E-4
28	4.0E-3	1.7E-3	2.5E-3	3.2E-3	2.1E-3	1.0E-3
35	4.5E-3	1.9E-3	2.8E-3	3.6E-3	2.3E-3	1.4E-3
65	4.8E-3	2.2E-3	3.1E-3	3.9E-3	2.6E-3	1.7E-3
95	5.1E-3	2.4E-3	3.4E-3	4.2E-3	2.9E-3	2.0E-3

4.7.6.2. Soxhlet rapid leaching test.

In this investigation, the leaching rates of Cs^{+}, Co^{2+} and Eu^{3+} from different solidified waste forms have been determined **(Mastsuzyrn 1978)**. The results obtained are listed in Table (38).

The results obtained show that, the amounts leached of cesium, cobalt, and europium from this process are greater than that leached from the long term process, which indicate that temperature affects the leaching rate. It was also found that, the paste of plain OPC alone has a maximum leaching rate for cesium, cobalt and europium while the pastes of OPC mixed with homra, fly ash, silica fume, ceramic or window glass have lower leaching values . This may be attributed to the good filling properties of these solids that reduce the value of total porosity and decreased the leaching rates **(Faucon et al 1996)**.

When the additives were added to the OPC the leaching rate decreased in the following sequence:

OPC > (OPC+S.F) > (OPC+F.A) > (OPC+C) > (OPC+H) > (OPC+W.G).

It was also found that Eu (152+154) has the lowest values which may be explained its strong reaction with the solids and Cs-137 has the highest corresponding values as it may react weakly with the solids. The leaching rate for the investigated radioisotopes took the following order Cs^{+}> Co^{2+} > Eu^{3+} **(Crawford and Rahman 1984)**.

Table (38): The soxhlet rapid leaching rates of ^{137}Cs, ^{60}Co and $^{(152+154)}Eu$ mixed with portland cement and portland cement mixed with the industrial solid materials.

Compositions	Leaching rate, (gm cm^{-2} d^{-1})		
	Cs^{+}	Co^{2+}	Eu^{3+}
Plain OPC	8.3E-2	6.1E-2	9.6E-3
OPC+ homra	3.1E-2	1.3E-2	2.1E-3
OPC+ fly ash	5.6E-2	4.4E-2	6.9E-3
OPC+ silica fume	7.2E-2	5.3E-2	7.2E-3
OPC+ ceramic	4.3E-2	2.7E-2	4.3E-3
OPC+ window glass	3.7E-3	9.8E-3	1.1E-3